CLOUD PROCESSING OF INTERNAL MIXED AEROSOL: A NUMERICAL STUDY 2.2 USING A BIN AEROSOL-MICROPHYSICS SCHEME COUPLED WITH WRF

Lulin Xue[1]*, István Geresdi[2] and Roy Rasmussen[1]
1. National Center for Atmospheric Research, Boulder, CO
2. University of Pécs, Pécs, Hungry

1. INTRODUCTION

By acting as cloud condensation nuclei (CCN) and ice nuclei (IN), atmospheric aerosols exert great impacts on clouds, precipitation and the climate system. Meanwhile, aerosols are modulated by clouds and precipitation. Processed and transported by clouds, aerosols are redistributed in the air through scavenging (sink) and evaporation (source). Their chemical and hygroscopic features are changed by clouds as well (Flossmann 1997). These redistributed and modified aerosols affect radiation transfer, clouds, precipitation and their subsequent developments (Hatzianastassiou et al. 1998; Wurzler et al. 2000).

Xue et al. (2010) pointed out the importance of representing aerosol regeneration process in the models to simulate cloud and precipitation more accurately. By performing various sensitivity tests, they found that aerosol chemical compositions have relatively great impact on clouds and precipitation when the aerosol solubility is very low and when the updraft is weak, which is in agreement with the results of Reutter et al. (2009). They also found that the secondary cloud and precipitation are sensitive to regenerated aerosol size distributions and solubility under certain conditions.

Although the possible effects of cloud-processed aerosols on clouds and precipitation have been explored by Xue et al. (2010), the details of cloud processing and properties of regenerated aerosols were not thoroughly represented in their model. A new bin aerosol-microphysics scheme has been developed and coupled into the Weather Research and Forecast model (WRF) to tackle this problem.

By simulating 2D orograhic clouds in a periodic boundary domain, this study examined how aerosols are processed by clouds under three background concentrations and two moist conditions and the effects of these processed aerosols on precipitation.

* *Corresponding author address: Lulin Xue, National Center for Atmospheric Research, Boulder, CO 80301; e-mail: xuel@ucar.edu*

2. MODEL DESCRIPTIONS

The scheme used in this study was developed based on the one presented in Geresdi and Rasmussen (2005). In this new scheme, the aerosol particles are assumed to be internal mixtures of ammonia sulfate and dust, where ammonia sulfate represents soluble material and dust represents insoluble part. Thirty six bins covering radius from 0.012 to 65 μm are used to describe the dry aerosol number concentration, mixing ratios of soluble and insoluble materials. Dry deposition or scavenging of super-micron aerosols is considered in the scheme.

The method documented in Khvorostyanov and Curry (2007) of calculating equilibrium radii of partially soluble aerosols under sub-saturation condition was used to initialize haze particles and drops in the scheme. There are 55 mass doubling bins in total to illustrate the haze and drop number concentration, mixing ratio, soluble and insoluble aerosol mixing ratios inside drops, in which the first 19 bins are dedicated to haze category while the others are for cloud drops. The spectrum covers 0.02 μm to 8 mm in radius for haze and drop.

After haze particles or drops are formed in the model, the solute effect and the curvature effect are both considered in the diffusional growth process (Geresdi and Rasmussen 2005). When drops evaporate, the aerosol mass inside them is released back into the air. All aerosol mixing ratios inside/outside the drops are tracked and conserved.

The method of moments (Tzivion et al. 1987; Reisin et al. 1996) are used for the collision-coalescence of cloud drops and the Brownian, the thermophoretic and the gravitational collections of dry aerosols and haze particles by cloud drops to conserve the number and mass for dry aerosols and drops. The binary breakup process induced by collision is not considered in the scheme to avoid numerical difficulties of partitioning aerosol mass into separate drops.

This scheme has been implemented into WRF version 3.1. At current stage, the aqueous chemistry and ice-phase microphysical processes are not included in the scheme.

3. EXPERIMENTAL DESIGN

A similar model setup as the one in Xue et al. (2010) was applied in this study. The 2D domain consists of 300 grid points with a resolution of 500 m. A bell-shape mountain is located in the center of the domain. The vertical coordinate, mountain shape and soundings are the same as in Xue et al. (2010) except that 90% and 75% surface relative humidities are used here instead of 95% and 85% (Fig. 1).

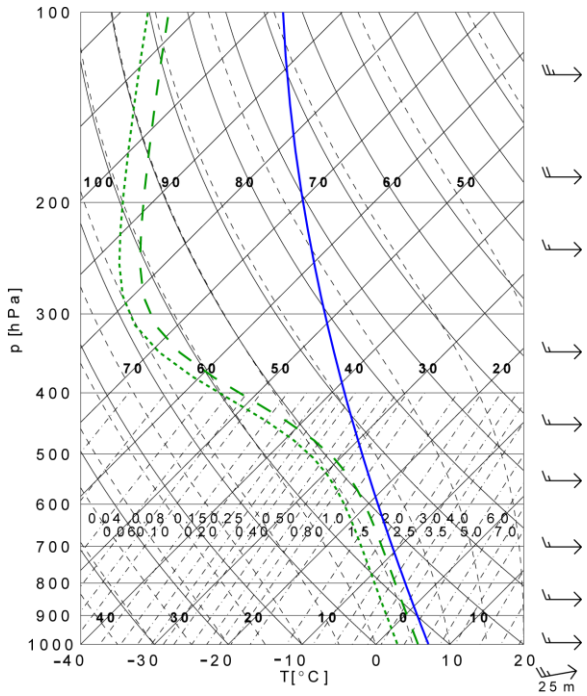

Fig. 1. The soundings for the simulations. The blue line indicates temperature (T) with a surface T of 280.15 K. The long dashed green line indicates the dewpoint T with 90% surface relative humidity (RH). The short dashed green line is the dewpoint T with 75% surface RH.

The aerosol initial backgrounds are prescribed as maritime (M), remote continental (RC) and urban (U) according to Jaenicke (1998) (Fig. 2).

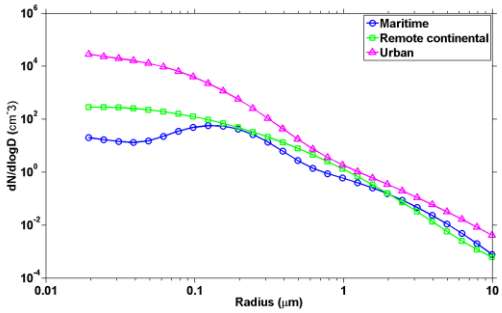

Fig. 2. Background aerosol size distributions (maritime, remote continental, and urban).

In order to investigate how clouds modified aerosol solubility after processing, three different solubility distributions described by Eq. (1) – (3) are tested.

$$FC = \begin{cases} 1 & r \le 5\times10^{-8} \\ 1.13\times e^{-2.5\times10^{6}\times r} & 5\times10^{-8} < r \le 1\times10^{-6} \\ 5\times10^{-10}\times r^{-1.382} & 1\times10^{-6} < r \le 5\times10^{-6} \\ 0.01 & r > 5\times10^{-6} \end{cases} \quad (1)$$

$$FC1 = \begin{cases} 1 & r \le 5\times10^{-8} \\ 0.5 & 5\times10^{-8} < r \le 1\times10^{-6} \\ 0.25 & 1\times10^{-6} < r \le 5\times10^{-6} \\ 0.1 & r > 5\times10^{-6} \end{cases} \quad (2)$$

$$FC2 = \begin{cases} 0.1 & r \le 5\times10^{-8} \\ 0.2 & 5\times10^{-8} < r \le 1\times10^{-6} \\ 0.5 & 1\times10^{-6} < r \le 5\times10^{-6} \\ 1 & r > 5\times10^{-6} \end{cases} \quad (3)$$

Here, r is aerosol radius in m. The initial aerosol was truncated at 10 μm. The solubility distributions are illustrated in Fig. 3.

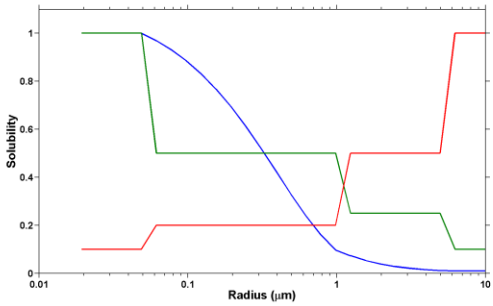

Fig. 3. Aerosol solubility distributions. The blue line indicates FC. The green line is FC1 and the red line is FC2.

The lateral boundary condition was set to periodic to simulate continuous orographic cloud formation in a small domain. Because precipitation from the clouds depletes total water vapor, a uniform surface latent heat flux of 25 W m^{-2} (10 W m^{-2}) was prescribed for RH=90% (75%) case to compensate the vapor loss. Sensible heat flux was set to 2 W m^{-2}. All cases were run for 12 hours to simulate 3 cloud processing cycles. The experiments are listed in Table 1.

Table 1. List of experiments

	FC	FC1	FC2
M_RH90	X		
M_RH75	X		
RC_RH90	X	X	X
RC_RH75	X	X	X
U_RH90	X		
U_RH75	X		

"X" indicates a combing case has been performed.

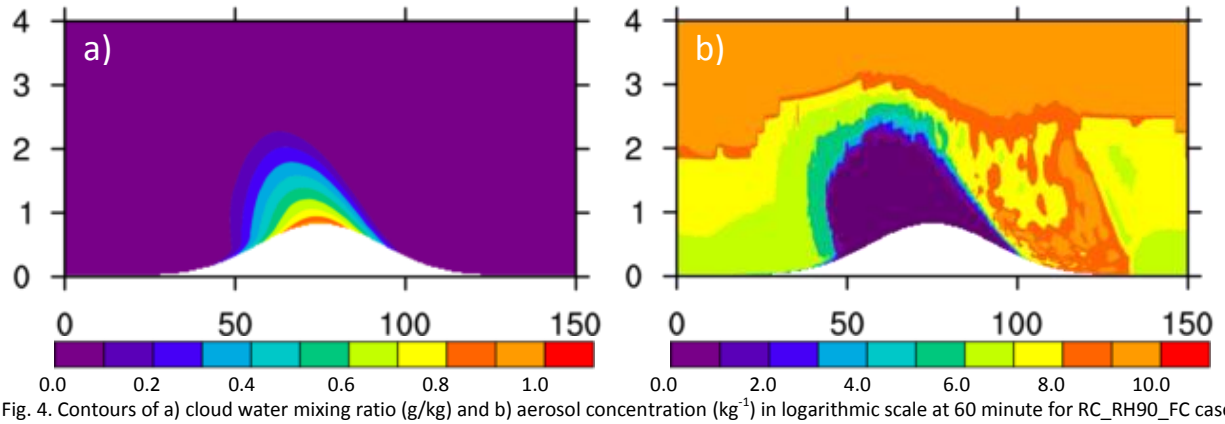

Fig. 4. Contours of a) cloud water mixing ratio (g/kg) and b) aerosol concentration (kg^{-1}) in logarithmic scale at 60 minute for RC_RH90_FC case.

4. RESULTS

Figure 4 illustrates snapshots of cloud water mixing ratio and dry aerosol number concentration at 60 minute for RC_RH90_FC case. At this moment, the orographic cloud top reached about 2.5 km with a maximum mixing ratio of 0.8 g/kg. As expected, the aerosol concentration within cloud area is very low (<10 kg^{-1}) which represents interstitial aerosols. On the other hand, the concentration of regenerated aerosols behind the leeward edge of the cloud is relatively high (> 10^6 kg^{-1}) which reflects the strong evaporation associated with the cloud. The features of cloud-processed aerosols and their effects on precipitation are analyzed in the following sections.

4.1 *Bulk Solubility of Cloud-processed Aerosols*

We define aerosol bulk solubility as the ratio between domain-integrated soluble aerosol mass in the air (both dry and in-drop aerosol mass) and domain-integrated total aerosol mass in the air. Figure 5a shows that for FC solubility distribution, the bulk solubility of each background increases with time. This result can be explained by the facts that 1) aerosol mass in the air is the difference between initial aerosol mass and that being scavenged onto the ground (there is no aerosol source in the domain); 2) for FC, most insoluble mass is associated with large aerosols (see Fig. 3) which are easier to be removed by nucleation, impact and dry scavenging; 3) more insoluble mass is removed than soluble mass which leads to more soluble mass in the air and higher bulk solubility. Therefore, we expect that bulk solubility decreases with time for FC2 cases since more soluble aerosol mass is scavenged than insoluble mass, which is confirmed by Fig. 5b. A conclusion can be drawn based on previous analyses that the solubility of large aerosols decides the aerosol bulk solubility after cloud processing.

4.2 *Size Distribution and Solubility Distribution of Cloud-processed Aerosols*

Unlike the arbitrarily prescribed size and solubility distribution in Xue et al. (2010), the size distribution and solubility distribution of regenerated aerosols in this study are predicted by the scheme. Figures 6 and 7 illustrate the size distributions and solubility distributions of cloud-processed aerosols at 30 minute, 3 and 12 hour for M_RH75_FC, RC_RH75_FC and U_RH75_FC cases.

As Fig. 6 shows, aerosols greater than 10 μm were

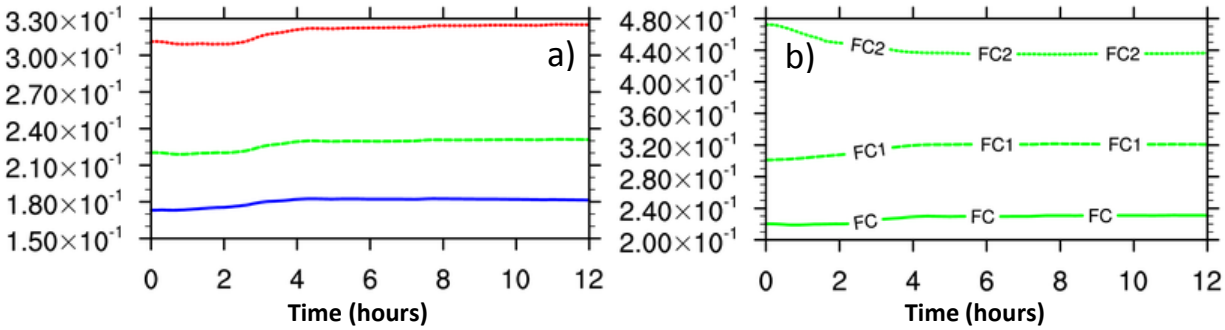

Fig. 5. Time series of aerosol bulk solubility for a) M_RH75_FC (blue), RC_RH75_FC (green), and U_RH75_FC (red) cases and b) RC_RH75_FC, RC_RH75_FC1, and RC_RH75_FC2 cases.

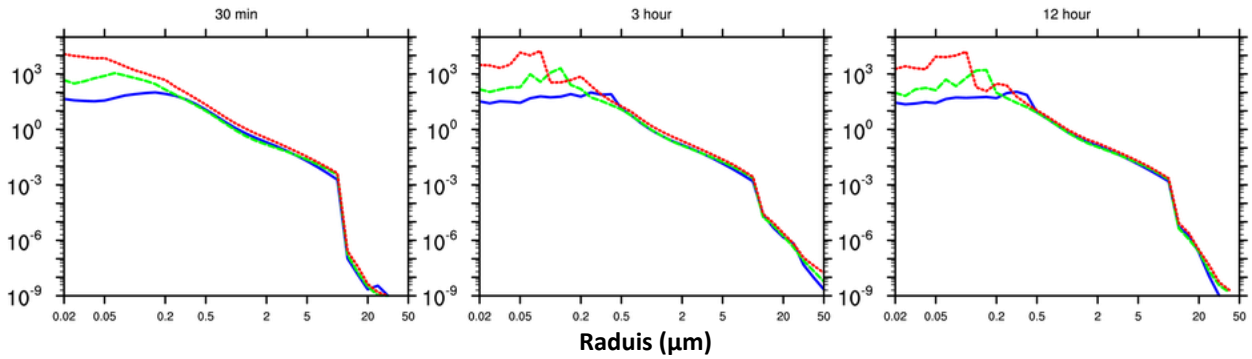

Fig. 6. Size distributions of cloud-processed aerosols of M_RH75_FC (blue), RC_RH75_FC (green) and U_RH75_FC (red) at three time steps.

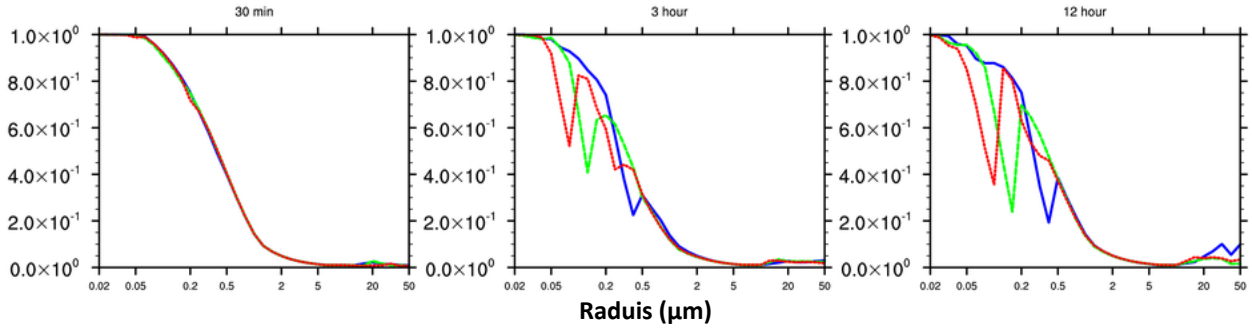

Fig. 7. Solubility distributions of cloud-processed aerosols of M_RH75_FC (blue), RC_RH75_FC (green) and U_RH75_FC (red) at three time steps.

generated by cloud-processing which were not available at the beginning of the simulations (initial size was truncated at 10 μm). The growth of aerosols is the result of combination of aerosols in different drops by the collision-coalescence process. It is also noticed that the size distributions of regenerated aerosols at 3 hour resemble those at 12 hour very closely. This indicates that after several cloud processing cycles, the size distribution of processed aerosols will reach an equilibrium state.

Figure 7 shows that for different aerosol backgrounds, the sizes of aerosols whose solubility are modified most significantly are different. However, there is a common feature for all backgrounds that the newly generated large aerosols (> 10 μm) have higher solubility than those between 5 and 10 μm. This finding is in agreement with previous studies (Flossmann 1997; Wurzler et al. 2000).

The evolutions of the solubility distributions of RC_FC, RC_FC1 and RC_FC2 cases under dry and wet conditions are described in Fig. 8. For FC and FC1 distributions, solubility of small size aerosols reduces and that of newly formed large aerosols increases. It is opposite for FC2 distribution.

In summary, cloud processing generates larger aerosols, equilibrates the aerosol size distribution and smoothes the aerosol solubility distribution.

4.3 *Effects of Cloud-processed Aerosols on Precipitation*

The effects of cloud-processed aerosols on precipitation are illustrated in Fig. 9. F1 indicates that all the aerosols in the domain are 100% soluble ammonia sulfate. Under both dry and wet conditions, each solubility distribution has similar effect on precipitation formation before regenerated aerosols enter the cloud (before 3 hr). FC2 always generated

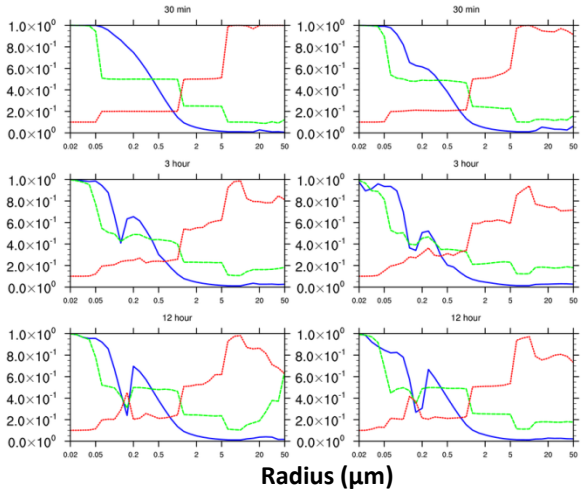

Fig. 8. Solubility distributions of cloud-processed aerosols of RC_FC (blue), RC_FC1 (green), and RC_FC2 (red) under RH=75% (left) and RH=95% (right) at three time steps.

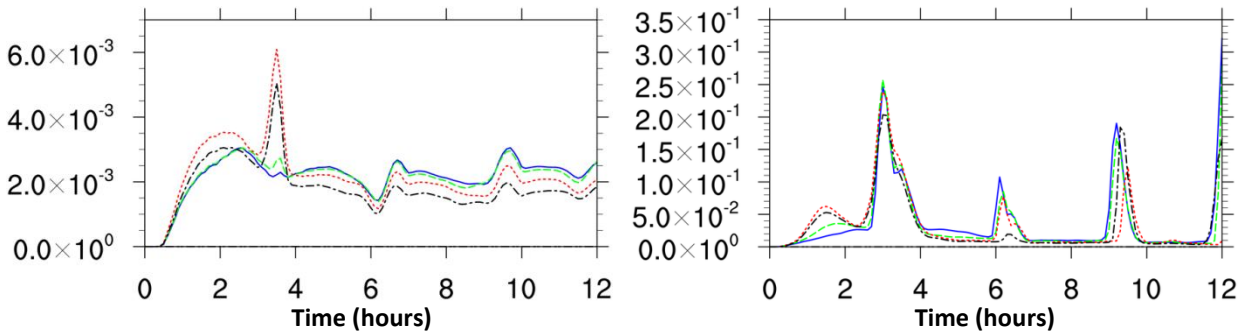

Fig. 9.Time series of precipitation rate (mm/h) of RC_FC (blue), RC_FC1 (green), RC_FC2 (red), and RC_F1 (black) with a) RH=75% and b) RH=90%.

strongest precipitation before 3 hour. F1 generated weaker precipitation than FC2 but stronger than FC and FC1. The spikes in Fig. 9 are associated with the advected updraft originated from wave breaking region, which indicate the cycle number. Interestingly, FC2 and F1 generated weaker precipitation than FC and FC1 after the first cycle. However, FC2 was still stronger than F1. The nonlinear response of precipitation rate to cloud-processed aerosols with different solubility distributions reflects the complexity of aerosol-cloud-precipitation interaction. To explain such phenomena, further analyses are required.

5. SUMMARY

A new detailed bin aerosol-microphysics scheme has been developed to investigate cloud processing of internal mixed aerosols. A series of idealized 2D simulations of orographic clouds have been conducted using this scheme coupled with WRF model. The results showed that 1) the solubility of large aerosols decides the aerosol bulk solubility after cloud processing; 2) cloud processing generates larger aerosols, equilibrates the aerosol size distribution and smoothes the aerosol solubility distribution; 3) cloud-processed aerosols have complicated effects on clouds and precipitation.

ACKNOWLEDGEMENTS

This study was partly supported by NCAR Advanced Study Program (ASP), the Presidency of Meteorology and Environment (PME) in Saudi Arabia through a contract with Weather Modification Incorporate (WMI) of Fargo, North Dakota, and the Wyoming Weather Modification Pilot Program.

REFERENCES

Flossmann, A. I., 1997: Interaction of aerosol particles and clouds. *J. Atmos. Sci.*, **55**, 879-887.

Geresdi, I. and R. M. Rasmussen, 2005: Freezing drizzle formation in stably stratified layer clouds. Part II: The role of giant nuclei and aerosol particle size distribution and solubility. *J. Atmos. Sci.*, **62**, 2037-2057.

Hatzianastassiou, N., W. Wobrock and A. I. Flossmann, 1998: The effect of cloud-processing of aerosol particles on clouds and radiation. *Tellus*, **50B**, 478-490.

Jaenicke, R., 1998: Aerosol physics and chemistry. *Physical and Chemical Properties of the Air.* Vol. 4b, *Numerical Data and Functional Relationships in Science and Technology*, G. Fischer, Ed., Landolt-Bomstein New Series, Springer, 391-457.

Kvorostyanov, V. I. and J. A. Curry, 2007: Refinements to the Kohler's theory of aerosol equilibrium radii, size spectra, and droplet activation: Effects of humidity and insoluble fraction. *J. Geophys. Res.,* **112**, D05206.

Reisin, T., Z. Levin, and S. Tzivion, 1996: Rain production in convective clouds as simulated in an axisymmetric model with detailed microphysics. Part I. Description of the model. *J. Atmos. Sci.,* **53**, 497-519.

Reutter, P., and Coauthors, 2009: Aerosol- and updraft-limited regimes of cloud droplet formation: influence of particle number, size and hygroscopicity on the activation of cloud condensation nuclei (CCN). *Atmos. Chem. Phys.*, **9**, 706707080.

Tzivion, S., G. Feingold, and Z. Levin, 1987: An efficient numerical solution to the stochastic collection equation. *J. Atmos. Sci.,* **44**, 3139-3149.

Wurzler, S., T. G. Reisin, and Z. Levin, 2000: Modification of mineral dust particles by cloud processing and subsequent effect on drop size distributions. *J. Geophys. Res.*, **105**, 4501-4512.

Xue, L., A. Teller, R. Rasmussen, I. Geresdi, and Z. Pan, 2010: Effects of Aerosol Solubility and Regeneration on Warm-phase Orographic Clouds and Precipitation Simulated by a Detailed Bin Microphysical Scheme. *J. Atmos. Sci.*, DOI: 10.1175/2010JAS3511.1.